European Journal of Phycology

ISSN: 0967-0262 (Print) 1469-4433 (Online) Journal homepage: http://www.tandfonline.com/loi/tejp20

Phylogeny, species diversity and biogeographic patterns of the genus Tricleocarpa (Galaxauraceae, Rhodophyta) from the Indo-Pacific region, including T. confertus sp. nov. from Taiwan

Shao-Lun Liu, Showe-Mei Lin & Pin-Chen Chen

To cite this article: Shao-Lun Liu, Showe-Mei Lin & Pin-Chen Chen (2015) Phylogeny, species diversity and biogeographic patterns of the genus Tricleocarpa (Galaxauraceae, Rhodophyta) from the Indo-Pacific region, including T. confertus sp. nov. from Taiwan, European Journal of Phycology, 50:4, 439-456, DOI: 10.1080/09670262.2015.1076892

To link to this article: http://dx.doi.org/10.1080/09670262.2015.1076892

Eur. J. Phycol. (2015), **50**: 439–456

Phylogeny, species diversity and biogeographic patterns of the genus *Tricleocarpa* (Galaxauraceae, Rhodophyta) from the Indo-Pacific region, including *T. confertus* sp. nov. from Taiwan

SHAO-LUN LIU[1], SHOWE-MEI LIN[2] AND PIN-CHEN CHEN[1]

[1]*Department of Life Science, Tunghai University, Taichung 40704, Taiwan*
[2]*Institute of Marine Biology, National Taiwan Ocean University, Keelung 20224, Taiwan*

(Received 21 October 2014; revised 22 March 2015; accepted 28 March 2015)

Among four different genera in Galaxauraceae, species diversity of the genus *Tricleocarpa* Huisman & Borowitzka is underestimated and requires further examination. In this study, we explored a molecular phylogeny of *Tricleocarpa* with an emphasis on Taiwan species and reassessed species diversity of the genus from the Indo-Pacific region based on analyses of *rbc*L and COI-5P sequences and morphological observations. The molecular analyses showed that species of *Tricleocarpa* examined are grouped into seven clades: six clades in the *T. cylindrica* group (the *T. cylindrica* complex, *T. confertus, T. jejuensis, T. natalensis* and two uncharacterized *T.* '*cylindrica*' clades) and one clade as the *T. fragilis* group. Overall, at least 12 species in *Tricleocarpa* were detected from the Indo-Pacific region, including a new species, *T. confertus* S.-L. Liu & S.-M. Lin, from Taiwan. Among them, *T. confertus* can be separated from other species of *Tricleocarpa* by a thallus consisting of dichotomous or trichotomous, articulated and moniliform branches with smooth surfaces, constrictions at nodes and slightly anti-triangular in shape. The cystocarp morphology of *T. confertus* is similar to the *T. cylindrica* group by having paraphyses intermixing with gonimoblast filaments. Recognition of this new species from other species is also supported by the DNA-based, algorithmic species delimitation approaches. With the combination of molecular phylogeny and species diversity reassessment, our phylogeographic analysis supported a trend that species in the *T. fragilis* group are restricted in their distribution to subtropical and tropical areas whereas species in the *T. cylindrica* group have a wide distribution, ranging from temperate through to tropical areas.

Key words: DNA-assisted species identification, phylogeny, Galaxauraceae, integrative taxonomy, morphology, Taiwan, *Tricleocarpa confertus* S.-L. Liu & S.-M. Lin

INTRODUCTION

Members of the calcified red algal family Galaxauraceae (Rhodophyta) are widely distributed in temperate to tropical regions worldwide (e.g. Abbott, 1999; Huisman, 2006). The Galaxauraceae currently consists of four different genera including *Actinotrichia* Decaisne, *Dichotomaria* Lamarck, *Galaxaura* Lamouroux, and *Tricleocarpa* Huisman & Borowitzka, which was once regarded as belonging to *Galaxaura* and exhibits a much higher variation of branch width and thallus height among samples than the other three genera (Huisman *et al*., 2004; Huisman, 2006). Papenfuss & Chiang (1969) and Papenfuss *et al*. (1982) proposed *Galaxaura oblongata* Ellis & Solander [= *Tricleocarpa fragilis* (Linnaeus) Huisman & Townsend] as the only valid name circumscribing all species described in Decaisne's section *Eugalaxaura* (Kjellman, 1900). Later, the Decaisne's section *Eugalaxaura* was shown to contain more than one species and should be regarded as members of *Tricleocarpa* (Svedelius, 1945; Wiriyadamrikul *et al*., 2013*a*). When Huisman & Borowitzka (1990) established their new genus, *Tricleocarpa*, they only recognized two species [*T. cylindrica* (Ellis & Solander) Huisman & Borowitzka, and *T. oblongata* (Eliis & Solander) Huisman & Borowitzka (= *T. fragilis*)] and sunk many species of *Galaxaura* from Australia into these two species based on a broader species definition that allows wider morphological variations. Four species are currently recognized in *Tricleocarpa* including *T. cylindrica, T. fragilis*, and the two new species *T. jejuensis* and *T. natalensis* established by Wiriyadamrikul *et al*. (2013*a*), in which the authors revealed that the interspecific genetic diversity of *Tricleocarpa* is high using two genetic markers, plastid-encoded *rbc*L (the large subunit of RuBisCO) and mitochondria-encoded COI-5P (5' end of cytochrome c oxidase I). Their molecular analyses suggested that *Tricleocarpa* should comprise more species than currently recognized.

Correspondence to: Shao-Lun Liu. (e-mail: shaolunliu@thu.edu.tw)

ISSN 0967-0262 (print)/ISSN 1469-4433 (online)/15/040439-456 © 2015 British Phycological Society
http://dx.doi.org/10.1080/09670262.2015.1076892

Identifying species using morphological traits is time-consuming and delays the exploration of biodiversity in genetically hyperdiverse but morphologically similar biological groups. Recently, the DNA-assisted species delimitation approach has been shown to be an effective approach to determine the species boundary in a phylogenetic tree (i.e. the phylogenetic species concept; reviewed in Leliaert *et al*., 2014). Since the gene flow of speciation process was expected to produce separated discontinued genetic groups that are considered as the putative species or evolutionarily significant units (ESUs) (e.g. Verbruggen *et al*., 2007), several statistical algorithms have been developed to assist the determination of the species boundary based on single-locus molecular data, such as the Generalized Mixed Yule-Coalescent (GMYC) model method (Pons *et al*., 2006), the statistical parsimony network (SPN) method (e.g. Hart & Sunday, 2007), and the automatic barcode gap discovery (ABGD) method (Puillandre *et al*., 2012). These statistical methods have been proved to coincide with the Linnaean names and often reveal cryptic species diversity in seaweeds (reviewed in Leliaert *et al*., 2014). The outcome of the single-locus algorithm-based species delimitation can then be validated by the analysis of multilocus sequences using a popular Bayesian multilocus validation method (Bayesian Phylogenetics and Phylogeography; BPP) (e.g. Carstens *et al*., 2013; Payo *et al*., 2013). Complementary to morphological traits, the integration of statistical algorithms for the species determination could be regarded as the integrative taxonomy approach (Schlick-Steiner *et al*., 2010).

During a continuous sampling effort of species of Galaxauraceae in Taiwan since 2003, the second author found an unusual *Tricleocarpa* species that was morphologically distinct from all known *Tricleocarpa* species by possessing articulated and moniliform branches, which had not been found in any known species in the genus. In this study, we used a molecular approach to infer the taxonomic status and phylogenetic affinity of this alga along with other species of *Tricleocarpa* based on two commonly used DNA barcodes in red algae – *rbc*L and COI-5P (Saunders & Moore, 2013). In addition to the morphological observations, several algorithmic methods (viz. GMYC, SPN, ABGD and BPP) were applied for a validation of the taxonomic status of our new finding in relation to other species in the genus. Overall, the goals of this study are fourfold. First, the molecular phylogeny of *Tricleocarpa* was reassessed based on two genetic markers, *rbc*L and COI-5P. Second, the number of putative species (= ESUs) of *Tricleocarpa* from the Indo-Pacific region was explored based on different algorithmic methods. Third, we characterized a new species, *T. confertus*, morphologically and examined its molecular taxonomy and phylogenetic affinity using an integrative taxonomy approach. Fourth, we provided the biogeographic patterns of *Tricleocarpa* based on the analytical results of molecular phylogeny and the algorithmic species delimitation.

MATERIALS AND METHODS

Sample collection and morphological observations

Specimens were collected by scuba diving. After collection, a small portion of sample was preserved in silica-gel for molecular analyses and the rest of the sample was preserved in 5–10% formalin in seawater for morphological observations. Voucher specimens are deposited at the Herbarium of Tunghai University (TUNG), Taichung, Taiwan. For morphological observations, distal ends or young parts of branches were decalcified with a 1N HCl solution and then either squashed or sectioned by hands using a double-sided razor blade. Materials for morphological observations were stained with either a 1% aniline blue solution acidified with 1N HCl or an aceto-haematoxylin-chloral hydrate solution (Wittmann, 1965). Photographs were taken using a Canon EOS600D digital camera (Tokyo, Japan) mounted on a Leica DM750 light microscope (Frankfurt, Germany). Collection information is provided in the Supplementary Table S1.

Molecular analyses

Genomic DNA was extracted using the commercial ZR Plant/Seed DNA kit (Zymo Research, CA, USA) following the manufacture's manual. Analytical procedures of gene amplification and sequencing followed those described in Lin *et al*. (2001) and Wang *et al*. (2005). Gene-specific primers used for gene amplification and sequencing are listed in Freshwater & Rueness (1994), Lin *et al*. (2001), Geraldino *et al*. (2006), Yang *et al*. (2008) and Saunders & Moore (2013) as below: *rbc*L (F7/F160+R753, F492+R1150, and F993+RrbcSstart) and COI-5P (cox143F+C880R and GazF2+ GazR2). Two degenerated COI-5P primers designed specifically for *Tricleocarpa* are: 5'-TGTATGTCNYTVYTRATAAGAATGG-3' (tri.COI5P.F, forward primer) and 5'-TTAAAAGCATYGTTATTGCYCC-3' (tri.COI5P.R, reverse primer). DNA sequencing was carried out using an ABI3730 DNA Sequencer (Applied Biosystems, Foster, CA) at the Mission Biotechnology Company (Taipei, Taiwan). The newly generated sequences were available online for 13 *rbc*L sequences (GenBank accession numbers: KM494918 through KM494930) and for 12 COI-5P sequences (KM494931 through KM494942) (see Table S1). Additionally, 41 *rbc*L and 34 COI-5P sequences for *Tricleocarpa* as well as the selected outgroup (*Actinotrichia, Dichotomaria* and *Galaxaura*) were obtained from GenBank with accessions listed in Wang *et al*. (2005), Sherwood *et al*. (2010) and Wiriyadamrikul *et al*. (2013*a*, *b*).

Phylogenetic analyses

Two sets of DNA sequence alignments (i.e. *rbc*L and COI-5P dataset) were concatenated, resulting in a 2079

nucleotide alignment. Only sequences obtained from the same voucher specimens were concatenated. The best-fit nucleotide substitution model for the concatenated dataset was tested using the program PartitionFinder (Lanfear *et al*., 2012) with the following six different partition strategies: (1) single partition; (2) two partitions: *rbc*L and COI-5P; (3) three partitions: codon partition (cp) in 1-2-3 configuration; (4) two partitions: codon partition in 1-1-2 configuration; (5) six partitions: *rbc*L with cp in 1-2-3 configuration and COI-5P with cp in 1-2-3 configuration; and (6) four partitions: *rbc*L with cp in 1-1-2 configuration and COI-5P with cp in 1-1-2 configuration. The best partition strategy and model of sequence evolution were selected based on Bayesian Information Criterion (BIC). After determining the best-fitting nucleotide substitution model for the concatenated dataset, maximum likelihood (ML) trees of the concatenated alignment were inferred using the program RAxML v.7.0.4 (Stamatakis, 2006). Statistical support for each node of phylogenetic tree were computed using 1000 replicates of bootstrapping analyses (Felsenstein, 1985) with the ML method. The concatenated two-gene dataset was also subjected to Bayesian phylogenetic analyses using the software MrBayes v.3.2.1 (Ronquist *et al*., 2012). Two independent runs with four heated Metropolis-coupled Monte Carlo Markov Chains (MCMC) were implemented. Each run was run for 50 million generations with tree and data sampling frequency of every 5000 generations. 50% of the resulting Bayesian trees were discarded as the 'burn-in'. The posterior probability for each node of the consensus tree was obtained from the post-burn-in saved trees with the split frequency of standard deviation < 0.01. Maximum clade credibility (MCC) tree with node heights of target tree based on the post burn-in trees was produced using the software TreeAnnotator v.1.5.3.

Single-locus species delimitation

To obtain an initial number of hypothetical species of *Tricleocarpa* from the Indo-Pacific region for later validation using two-gene Bayesian species delimitation analysis, we statistically delimited species using *rbc*L and COI-5P and followed three methods based on the Generalized Mixed Yule-Coalescent (GMYC) model (Pons *et al*., 2006), the statistical parsimony network (SPN) method (Clement *et al*., 2000), and the automatic barcode gap discovery (ABGD) method (Puillandre *et al*., 2012). We analysed *rbc*L and COI-5P dataset separately as both genes have different mutation rates. Because some data are missing at the 5' and 3' ends in the aligned dataset, we pruned the COI-5P dataset down to 479 nucleotides. In the *rbc*L dataset, we removed six sequences (KM494918, KM494923~24, KM494926, and KM494929~30) because their missing data was greater than 30% of aligned length of the majority of sequences. We then pruned the dataset down to 1407 nucleotides. In GMYC, the species number was estimated using the R package SPLITS (Monaghan *et al*., 2009) in an ultrametric phylogenetic tree. Since the single threshold model outperforms the multiple threshold model in GMYC (Fujisawa & Barraclough, 2013), the single threshold model was used in this study. The species boundary was determined based on the transition point from the interspecific branching rate (the pure birth Yule model) and the intraspecific branching rate (the neural Coalescent model). The ultrametric phylogenetic tree was reconstructed according to the analytical procedure described in Payo *et al*. (2013). The ultrametric trees were obtained using Bayesian analyses using BEAST v.1.6.1 (Drummond & Rambaut, 2007) with the GTR+G+I model for the nucleotide substitution multiple correction and divergence times calculated under an uncorrelated lognormal relaxed molecular clock model with the pure birth Yule speciation process as prior (Drummond *et al*., 2006). The uniform prior with value 0 as a lower and 10 as an upper boundary was selected in the ucld-mean (= the mean of the branch rates under the uncorrelated lognormal relaxed molecular clock) parameter by following default settings. A total of 50 million generations was run under the MCMC analyses with a tree sampling period of 5000 generations. The convergence with the ESS value larger than 200 was diagnosed using the software Tracer v.1.5 (Rambaut & Drummond, 2007). The MCC tree generated based on the trees after convergence with node heights of target tree was produced using the software TreeAnnotator v.1.5.3 for the subsequent GMYC analysis. A SPN analysis was carried out using the program TCS v.1.21 (Clement *et al*., 2000). The number of substitutions connecting haplotypes in the networks was calculated according to the algorithm described in Templeton *et al*. (1992). The redundant haplotypes were removed using a custom-made Perl script (available upon request). The statistical significance that excludes the homoplastic changes was set to 95% based on the empirical species delimitation cutoff described in Hart & Sunday (2007). The ABGD analysis was implemented using the online ABGD analytical tool (http://wwwabi.snv.jussieu.fr/public/abgd/abgdweb.html; Puillandre *et al*., 2012). For both datasets, the pairwise distance matrix was estimated using the best-fit T92+G_5 nucleotide substitution model using MEGA v6.06 (Tamura *et al*., 2013). The ABGD method detects the putative species based on a series of prior thresholds (ranging between 0.001 and 0.1) for a gap in the pairwise distribution of genetic distance. The relative gap width (X) was set to 1. The gap could be considered as the threshold of the upper limit of intraspecific distances and the lower limit of interspecific distances. For each prior threshold test, the dataset was first divided into the primary putative species number based on a statistically inferred barcode gap. Then, the same division procedure was recursively applied to the groups obtained in the primary division, thereby refining the division of groups for the final putative species number. The results from the initial partition were demonstrated to be empirically congruent with morphological species (Puillandre *et al*., 2012) and other algorithm-based species delimitation methods (Kekkonen & Hebert, 2014). We therefore considered the outcome of the initial partition in this study. Clades derived from GMYC, SPN and ABGD would be considered as potential putative species (= ESUs) if they met the two criteria: (1) the clades were congruent across three different algorithm-based species delimitation methods in both *rbc*L and COI-5P analyses; and (2) the clades

were well supported in the individual gene trees based on the bootstrapping analyses from the ML inference and posterior probability from the Bayesian inference.

Two-gene species delimitation

Single locus data can be problematic for the algorithm-based species delimitation due to the incomplete lineage sorting that yields the incongruence between gene tree and species tree. To validate the number of hypothetical species determined by the single locus data, a multilocus Bayesian method (Bayesian Phylogenetics and Phylogeography; BPP) that accommodates the species (population) phylogeny and coalescent processes in extant and ancestral species was applied to examine the results of the single locus algorithmic species delimitation using the program BP&P v2.0 (Rannala & Yang, 2003; Yang & Rannala, 2010). The two-gene data (*rbc*L+COI-5P herein) was used as input for BPP, which implements Bayesian MCMC algorithm for analysis of sequence alignments from multiple loci and a user-supplied species tree (the guide tree). The MCMC analyses allowed us to search for more parameter space that included ancestral population size (θ), population divergence time (τ) and estimated distribution of gene trees from multiple loci. This method accommodates the species phylogeny as well as lineage sorting due to ancestral polymorphisms with the JC nucleotide substitution model as the correction for multiple hits of sequence evolution. For the guide tree estimation, specimens were *a priori* assigned to species based on the results of the COI-5P GMYC results in the RAxML analysis using the guide tree derived from the two-gene ML analysis. Five variables (ε_1~ε_5) are automatically fine-tuned following the instructions of BP&P (Rannala & Yang, 2003; Yang & Rannala, 2010). The prior distribution of θ and τ could have influence on the posterior probabilities for different models (Yang & Rannala, 2010). As suggested by Leaché & Fujita (2010), three different prior probability distributions (as 'prior' hereafter) were used to examine the effects of θ and τ on the posterior probabilities of speciation events along the guide tree: (1) large θ with the gamma prior G (1, 10) and deep τ with G(1, 10); (2) small θ with G(2, 2000) and shallow τ with G(2, 2000); and (3) large θ with G(1, 10) and shallow τ with G(2, 2000). The other divergence time parameters are assigned the Dirichlet prior (Yang & Rannala, 2010: equation 2). Each analysis is run at least twice to confirm consistency between runs. Two independent MCMC analyses were run for 100,000 generations with the 'burn-in' = 20,000. To further examine whether the GMYC analysis of the *rbc*L dataset might underestimate species diversity, we reran the BPP analyses with the TFC3 clade that were subdivided into multiple entities across different single locus algorithmic approaches.

Biogeographical analysis and the extrapolation of extant species diversity

The species distribution of *Tricleocarpa* (i.e. ESUs) in the Central Indo-Pacific region was analysed using two R packages, 'map' and 'mapdata' (http://www.r-project.org/). Coordinate of each locality was obtained from the Google map (https://www.google.com/maps/). Extrapolation of species richness in the Central Indo-Pacific region beyond the current sampling effort was estimated using the online program iNEXT (Hsieh *et al*., 2013). Two estimators, sample-size-based rarefaction and extrapolation and coverage-based rarefaction and extrapolation, were estimated by following the methods used in Colwell *et al*. (2012) and Chao & Jost (2012). The lower and upper limits of 95% confidence interval for the estimators were performed by using 100 replicates of bootstrapping analyses.

RESULTS

Two-gene phylogeny

The analysed data matrix included 1407 base pairs (bp) for *rbc*L and 672 bp for COI-5P with no indels in the DNA sequences. Using PartitionFinder (Lanfear *et al*., 2012), three partitions (= codon partition (cp) in 1-2-3 configuration) with GTR+G+I were selected as the best scheme in the maximum-likelihood (ML) phylogenetic inference (*lnL* = −8534.4442; BIC = 18176.6366). In the Bayesian phylogenetic inference, the best partition scheme and model of sequence evolution are (1) *rbc*L, cp1 with GTR+I; (2) *rbc*L, cp2 with JC; (3) *rbc*L, cp3 with HKY+G+I; (4) COI-5P, cp1 with GTR+G+I; (5) COI-5P, cp2 with F81+I; and (6) COI-5P, cp3 with GTR+G+I (*lnL* = −8437.7538; BIC = 18074.9315).

The tree topology derived from the ML method was not congruent with that of the Bayesian analysis. ML topology of the *rbc*L and COI-5P phylogeny alone was largely congruent with ML topology of the *rbc*L+COI-5P phylogeny but with weaker internode supports, whereas Bayesian topology of the *rbc*L phylogeny alone was similar to Bayesian topology of the *rbc*L+COI-5P phylogeny. The ML phylogenetic analysis showed that specimens from various locations around the world grouped into two main monophyletic lineages. The first monophyletic lineage consisted of six clades: the *T. cylindric*a complex (TCC hereafter), *T. jejuensis* (TJ hereafter), *T. confertus* (TC hereafter), *T. natalensis* (TN hereafter) and two uncharacterized *T.* '*cylindrica*' clades (UTC1 and UTC2 hereafter) (Fig. 1). Considering that the cystocarp features of the first monophyletic group are highly similar to the authentic *T. cylindrica*, the first monophyletic group was referred to as the *T. cylindrica* group (TCG hereafter). The second lineage consisted of a species complex referred to as the *T. fragilis* complex (TFC hereafter) (Fig. 1). The monophyletic grouping of different clades of the *T. cylindrica* group (TCG) however received no support from the bootstrapping analyses. Within TCC, the first clade (TCC1) with samples from various localities of the Central Indo-Pacific region was subdivided into four well-supported lineages: TCC1, TCC2, TCC3 and TCC4. As *T. cylindrica* was described based on the sample from the Caribbean Sea (type locality), TCC2 was considered as the authentic *T. cylindrica*. Otherwise indicated, specimens in TCG that have not been characterized were placed under *T.* '*cylindrica*'. The second clade (TJ) contained one

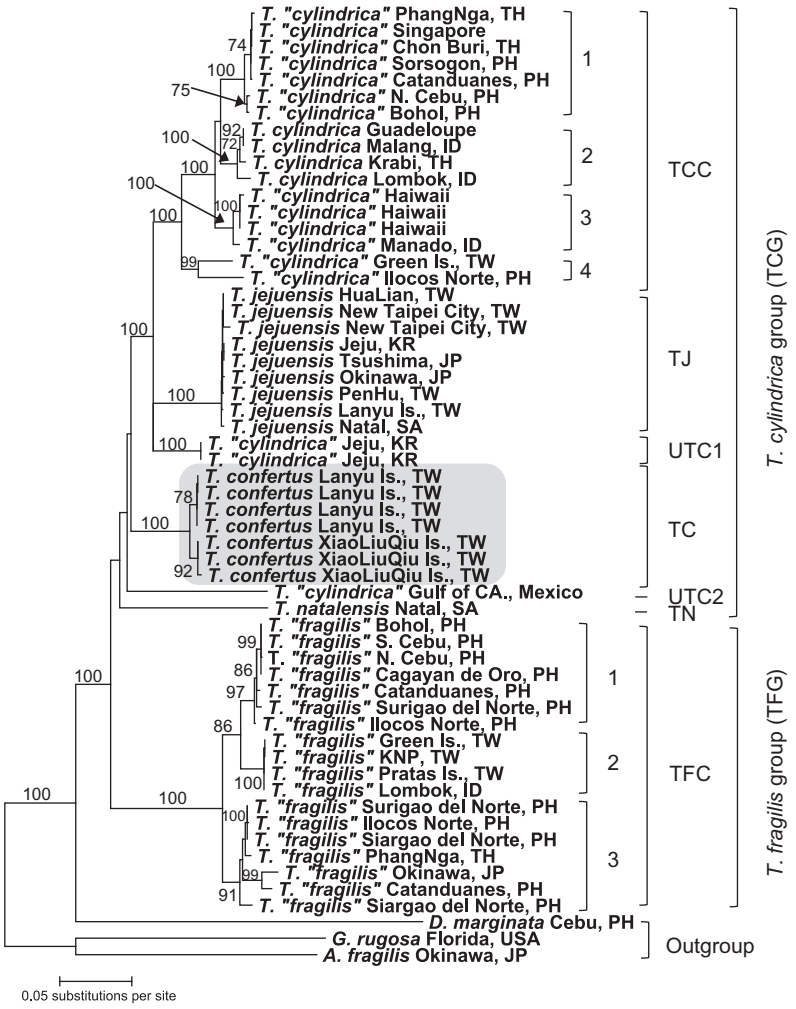

Fig. 1. Phylogram of concatenated *rbc*L and COI-5P of all available *Tricleocarpa* sequences based on the maximum likelihood inference. Bootstrap values from 1000 bootstrapping replicates of ML analyses (>70%) are shown on the branches. Scale bar indicates the number of nucleotide substitution per site. The new species is highlighted with the grey shading in colour.

species, *T. jejuensis*, from Korea, Japan and Taiwan. The third clade (UTC1) consisted of specimens from Korea that are as of yet characterized. The fourth clade (TC) consisted specimens from Taiwan, herein described as *T. confertus* sp. nov. based on algorithmic species delimitation and morphological evidence (see below). The fifth clade (UTC2) consisted of one specimen from the Gulf of California, Mexico. The basal clade (TN) consisted of one species, *T. natalensis*, from South Africa. In TFC, three well-supported lineages were recognized (Fig. 1): TFC1, TFC2 and TFC3. All specimens in TFC were from various localities in the Central Indo-Pacific region. Due to the lack of specimens from the type locality (Jamaica; Huisman & Townsend, 1993), the authentic *T. fragilis* remains uncertain at the moment. Similar to the ML tree, the Bayesian tree showed that *Tricleocarpa* species grouped into seven monophyletic assemblages with 12 distinct clusters (Supplementary Fig. S1). The main difference is that the *T. cylindrica* group (TCG) did not form a monophyletic group.

Algorithmic species delimitation

Our phylogenetic analyses suggested that the 12 clusters might correspond to 12 species (ESUs). To examine this assumption, we first obtained the number of the hypothetical species based on the single locus data and then applied a two-gene Bayesian species delimitation approach for the validation. In the single-locus analyses, both *rbc*L and COI-5P pruned alignments were subjected to the algorithmic species delineation using GMYC-, SPN- and ABGD-based methods. Results are summarized in Supplementary Tables S2–S3 and Fig. 2. The GMYC model determined 13 and 14 clusters for the *rbc*L and COI-5P trees (Supplementary Table S2; Fig. 2). Results of the COI-5P tree is more liberal than the *rbc*L tree with two additional GMYC lineages (i.e. TFC3a and TFC3b). Results of SPN analysis were largely congruent with the GMYC modelling, but showed more segregation in TFC3 (Fig. 2). Results of ABGD analysis are highly congruent with that from the GMYC- and SPN-based analysis (Fig. 2). The

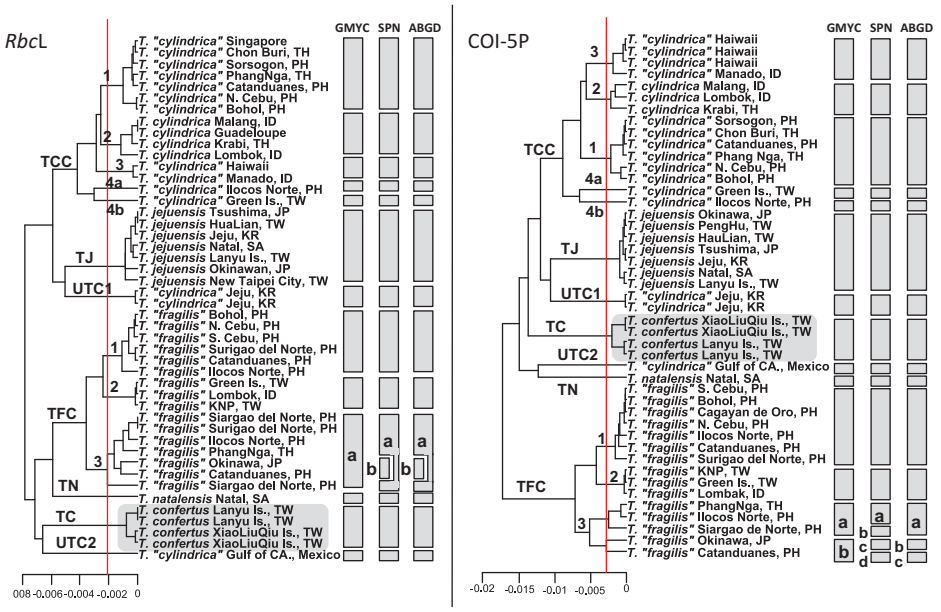

Fig. 2. Bayesian inference ultrametric gene tree obtained using a Yule tree prior in BEAST with the statistical species delimitation results from GMYC-, SPN- and ABGD-based algorithmic methods based on *rbc*L and COI-5P sequences. The columns to the right of trees indicate evolutionarily independent lineages obtained under GMYC-based (the first column), SPN-based (the second column) and ABGD-based (the third column) method. The new species is highlighted with the grey shading in colour. Red line indicates the maximum likelihood transition point of the branching rate from the interspecific to intraspecific processes by the GMYC model. Abbreviation: ABGD, Automated Barcode Gap Discovery; GMYC, Generalized Mixed Yule-Coalescent model; SPN, statistical parsimony network.

counts of ESUs varied from 7 to 21 with the lowest and highest results analysed by ABGD (Supplementary Table S3). ABGD analysis with the T92+G_5 nucleotide substitution model for the correction of multiple hits produced two initial partitions with ESU counts of 7 (P = 0.0077) and 14 (P = 0.0017) for the *rbc*L dataset and one initial partition with ESU counts of 15 (P = 0.0077) for the COI-5P dataset. Overall, results by ABGD analysis showed 14 and 15 ESUs for the *rbc*L and COI-5P datasets, respectively. When assessing the genealogical concordance across different analytical approaches with different datasets, 13 ESUs were concordantly retrieved, including TCC1~3, TCC4a~4b, TJ, TC, TN, UTC1~2 and TFC1~3 (Fig. 2).

To validate results of single-locus algorithmic species delineation, we applied the two-gene Bayesian species delimitation method with different guide trees that comprise different ESU numbers from single-locus species delimitation methods. When assuming that the genealogical concordant 13 ESUs correspond to species, the two-gene Bayesian species delimitation analysis supported high speciation probabilities in the guide tree despite the speciation between TCC4a and TCC4b being highly influenced by different prior probability distributions in the BPP analyses (Fig. 3). Furthermore, the two-gene Bayesian species delimitation did not support other guide trees for further subdivisions of TFC3 (insets in Fig. 3). Overall, the two-gene Bayesian analysis supported 12 well-supported ESUs (= species) that were consistent with the phylogenetic analyses.

Morphological descriptions

Based on the analytical results derived from different algorithmic species delimitation approaches using both *rbc*L and COI-5P datasets, it was evident that the articulated and moniliform *Tricleocarpa* from Taiwan was distinct from the four other described species of *Tricleocarpa*. Therefore, we proposed a new species, *T. confertus*, from Taiwan. Main morphological features including vegetative and reproductive structures are therefore described as below. Morphological comparative keys to all named *Tricleocarpa* species are given in Table 1.

***Tricleocarpa confertus* S.-L. Liu & S.-M. Lin sp. nov.** (Figs 4–35)

Diagnosis: Thalli up to 5.5 cm high, heavily calcified in cortex, pink in colour, main axes di- or trichotomously branched; branching intervals 4–15 mm long, branches terete, glabrous, slightly triangular in shape, constricted toward the internodes, 1.5–2.0 mm wide in upper portions and 1.0–1.8 mm in lower portions. Cortex composed of three to four layers of elongate and ovoid cells with slightly compressed innermost

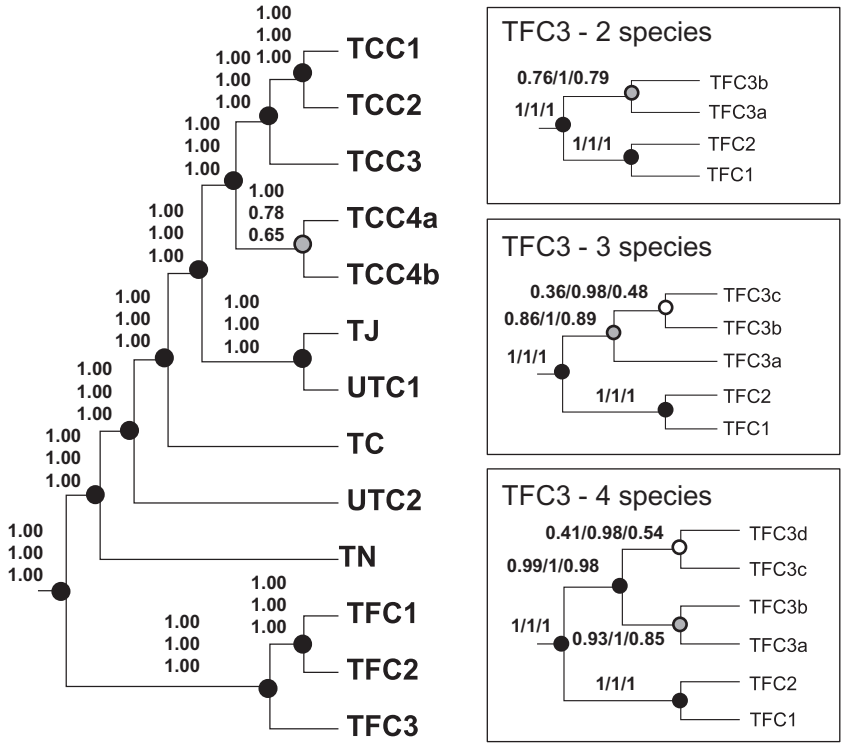

Fig. 3. The guide tree inferred from the concatenated *rbc*L and COI-5P dataset based on the maximum likelihood method. The speciation probabilities from the multi-locus Bayesian species delimitation results using BPP are shown on branches under three different combinations of priors: top, assuming large population sizes θ~G(1, 10) and deep divergences τ~G(1, 10); middle, assuming small population sizes θ~G(2, 2000) and shallow divergences τ~G(2,2000); bottom, assuming large populations sizes θ~G(1, 10) and relatively shallow divergences τ~G(2, 2000). Three insets indicate the multi-locus Bayesian speciation delimitation results after subdividing the third clade of the *T. fragilis* complex (= TFC3) into two species scenario (TFC3 – 2 species), three species scenario (TFC3 – 3 species), and four species scenario (TFC3 – 4 species). Strong supports by BPP (two out of three priors with $PP > 0.95$) are indicated by black circles, moderate to strong supports (two out of three priors: $0.75 < PP < 0.95$) are indicated by grey circles, and weak to moderate supports are indicated by white circles (two out of three priors with $PP < 0.75$).

cells. Gametophytes dioecious. Mature spermatangial conceptacle spherical, 200–250 μm in diameter, spermatangia obovoid, 5–6 μm in diameter. Each carpogonial branch composed of three cells: a carpogonium, a basal cell bearing several sterile filaments, and a hypogynous cell cut off at least three sterile branches with 3–5 larger cells with enlarged nuclei. Cystocarps hemispherical to spherical, 350–400 μm in diameter, gonimoblast filaments lining along inner walls of pericarps and mixing with paraphyses derived from pericarps. Carposporangia ovoid to obovoid, 30–35 μm wide by 50–75 μm long.

Holotype: TUNG14033.4 (Tunghai University Herbarium), collected at *c*. 8 m water depth on fringing reefs at Hou-Shi, XiaoLiuQiu, Pingtung Co., southern Taiwan, by S.-L. Liu, dated 15 February 2013.

Isotype: TUNG14033.5 (Tunghai University Herbarium), collected at *c*. 8 m water depth on fringing reefs at Hou-Shi, XiaoLiuQiu, Pingtung Co., southern Taiwan, by S.-L. Liu, dated 15 February 2013.

Type locality: HouShi fringing reef area, XiaoLiuQiu Island, Taiwan (22°19.270' N, 120° 21.484' E).

Etymology: The epithet *confertus* is Latin for 'constricted', referring the shape of branches.

Specimens examined: **Taiwan**: (1) Orchid Island, Taitung Co.: old KaiYuan Port, coll. S.M. Lin at *c*. 6 m water depth, 16 April 2002 (TUNG05025, female); coll. S.L. Liu & S.M. Lin at *c*. 6–20 m water depths, 6 April 2002 (TUNG05010, male). Ye-You, coll. S.L. Liu & S.M. Lin at *c*. 8 m water depth, 8 April 2003 (TUNG05151, female). (2) Hou-Shi fringing reef area, XiaoLiuQiu Island, Pingtung Co.: coll. S.L. Liu at *c*. 8–10 m water depths, 15 February 2013 (Males: TUNG14033.5, TUNG14033.12; females: TUNG14033.1 through TUNG14033.4, TUNG140334.6 through TUNG140334.11, TUNG140334.13, TUNG140334.14).

Distribution: Currently known only in Lanyu Island and XiaoLiuQiu Island, southern Taiwan.

Habitat and seasonality: Collections were made in February and April. The seasonality of *T. confertus* is unclear due to insufficient sampling. Plants grew on the coral reef in the subtidal area, in which the water depth is at least greater than 6 m.

Table 1. Comparison of morphological characters of all known *Tricleocarpa* species around the world.

Characters	*T. confertus*	*T. cylindrica*	*T. jejuensis*	*T. natalensis*	*T. fragilis*
Plant height (cm)*	2.5–5.5 (3.8 ± 0.8)*	*c.* 7.0	*c.* 8.7	*c.* 5.5	*c.* 10.0
Branch shape**	triangularly terete and moniliform	rectangularly terete	rectangularly terete	rectangularly terete	rectangularly terete
Branching pattern	dichotomous or trichotomous	dichotomous	dichotomous	dichotomous	dichotomous
Constricted branch	present	absent	absent	absent	absent
Branch length (cm)	0.4–1.5 (0.8 ± 0.3)	0.2–1.2	0.4–2.2	0.2–0.8	0.4–1.2
Branch width (mm)	upper: 1.5–2.0 (1.9 ± 0.2) lower: 1.0–1.8 (1.4 ± 0.3)	0.5–1.5	0.8–2.0	0.5–1.1	1.2–2.0
Degree of calcification	strong	strong	strong	strong	light
Cortical cell layer	three to four	three to four	three to four	three	three to four
Innermost cortex shape	elongate to compressed	compressed	elongate to compressed	elongate	compressed
Plant sexuality	dioecious	dioecious	monoecious	monoecious	dioecious or monoecious
Cystocarp diameter (μm)	350–400	250–350	250–400	200–250	400–500
Cystocarp shape	Spherical to hemispherical	hemispherical to slightly flattened	spherical	hemispherical	hemispherical to slightly flattened
Gonimoblast position	distributed along the inner face of cystocarp	distributed along the inner face of cystocarp	distributed along the inner face of cystocarp	distributed along the inner face of cystocarp	compact in the basal region of cystocarp
Paraphyses	intermixed with gonimoblast filaments	rarely intermixed with gonimoblast filaments	intermixed with gonimoblast filaments	rarely intermixed with gonimoblast filaments	not intermixed with gonimoblast filaments
Carposporangia dimension (μm)	50–70 × 30–35	18–30 × 10–15	20–30 × 10–15	15–30 × 10–15	55–70 × 25–40
Spermatangia conceptacle diameter (μm)	200–250	200–300	200–300	200–250	200–250
Spermatangia maximum diameter (μm)	5–6	5–8	5–8	5–7	5–8
Habitat	subtidal zones (> 6 m)	intertidal zones	intertidal or subtidal zones	intertidal zones	intertidal zones
Reference	This study	Wiriyadamrikul *et al.* (2013*a*)	Wiriyadamrikul *et al.* (2013*a*); this study	Wiriyadamrikul *et al.* (2013*a*)	Wiriyadamrikul *et al.* (2013*a*)

*Parentheses indicate mean and standard deviation from 14 different measurements.

**Bold font indicates the informative diagnostic characters for the separation between *T. confertus* and other *Tricleocarpa* species.

Habit. Thalli (Figs 4–5) are bushy and heavily calcified, 3–5.5 cm high, pale pink in colour in the field. Main axes are terete, moniliform, composed of erect dichotomously (Fig. 6) or occasionally trichotomously (Figs 7, 9) branches arising from a small discoid holdfast, 2–4 mm in diameter. Branches are constricted with internodes, 4–15 mm in length. The morphology of internodes is more or less triangular in shape, 1.5–2.0 mm wide at upper parts and 1.0–1.8 mm at lower parts of internodes (Fig. 8). Cortical layers are heavily calcified and are easily broken at nodes (Fig. 8), resulting in highly articulated branches (Fig. 9). Surface of branches is smooth without any assimilatory filaments. The vegetative growth of the thallus develops from the apical meristems (Fig. 10). Female and male reproductive structures are embedded in conceptacles with obvious ostioles scattering over surfaces of internodes of branches (Figs 11–12). In general, there are fewer female conceptacles in female specimens (Fig. 11) than male conceptacles in male plants (Fig. 12).

Vegetative structure. Except for the reproductive regions, calcification primarily occurs in the cortex (Figs 13–14), comprising three to four layers of cells, 60–70 μm thick (Fig. 16), whereas medullary filaments are loosely arranged, approximately 5 μm in diameter (Fig. 15). Outermost cortical cells are obpyramidal, 8–15 μm wide by 8–15 μm long in cross-section view, but appear to be polygonal, four to seven-sided in surface view (Fig. 17). Innermost cortical cells are rectangular, elongate, or slightly compressed, 25–35 μm wide by 25–40 μm long (Fig. 16), whereas cells in the middle layer of cortex are ovoid, 15–35 μm wide by 15–35 μm long.

Reproductive morphology. Gametophytes are dioecious and sexual structures are scattered over the thallus sunken in the cortex/medulla. Spermatangial branch initials are formed in place of ordinary cortical filaments near the apices of terete branches (Fig. 18) and divide laterally and transversely into several primary spermatangial filaments (Fig. 19) at early stages. As the growth continues, primarily spermatangial filaments divide laterally and distally to form hemispherical conceptacles, 200–250 μm in diameter when matured. Secondary spermatangial filaments are produced and grow toward inner cavities of the spermatangial conceptacles (Fig. 20). At maturity, spermatangia are 5–6 μm in diameter cutting off sub- or terminally from highly branched secondary spermatangial filaments (Fig. 21). Carpogonial branches are initiated, like spermatangial branch initials, in place of ordinary cortical filaments near apices of terete branches (Fig. 22). Carpogonial branch initials consist of three different cells, a basal cell, a hypogynous cell and a carpogonium terminated with a flask-shape trichogyne (Figs 22–23). The basal cell and hypogynous cell produce 3–4 sterile branches with 3–5 cells, which have similar cell size (Figs 24, 31–32). After presumably fertilization, the hypogynous cell enlarges, whereas the basal cell remains the same size. Meanwhile, numerous slender sterile filaments are produced from the basal cell of the carpogonial branch to form a pericarp (Figs 24, 32). At an early stage of carposporophyte development, the trichogyne degenerates and gradually disappears while the zygote divides transversely into two cells (Figs 25–26, 33–34). The lower cell cut off from the zygote functions as the gonimoblast initial which first divides obliquely to produce a young gonimoblast cell (Figs 27, 35), then subsequently develops into a carposporophyte. During cystocarp development, the short sterile branches (two to four cells long) are produced from the hypogynous cell but do not divide further and remain distinct (Fig. 28). On the other hand, several slender, sterile filaments are produced from the basal cell, and then surround the carpogonial branch and the gonimoblast filaments (Fig. 28). At maturity, numerous paraphyses (= involucral filaments) are produced from inner walls of conceptacles and intermix with gonimoblast filaments (Figs 28, 30). Pit plugs between cells of carpogonial branch break down, resulting in a multinucleate fusion cell; fully developed cystocarps are hemispherical to spherical, 350–400 μm in diameter (Figs 28–29). Mature carposporangia (Fig. 30) are ovoid or obovoid shaped, 30–35 μm wide by 50–75 μm long, produced singly and terminally from secondary gonimoblast filaments positioned at the centre of the cystocarp cavity (Fig. 29).

Distribution and biogeography

Species definition from our DNA-based, algorithmic analyses allowed us to reassess the geographic distribution of different *Tricleocarpa* species. We only evaluated the geographic range of the *Tricleocarpa* species in the Central Indo-Pacific region due to the sampling effort (i.e. the exclusion of UTC2 and TN): seven species in the *T. cylindrica* group (TCG) and three species in the *T. fragilis* complex (Fig. 36). Within TCG, *T. jejuensis* (TJ) is largely restricted to the northwestern Pacific region, suggestive of its preference in the temperate area. In addition, this species was also found in South Africa, indicative of its long-distance dispersal ability spanning the Indo-Pacific Ocean (Supplementary Table S4). TCC1 was largely distributed in the southeastern Asia oceanic area, spanning the Indo-Pacific Ocean (Supplementary Table S4). The authentic *T. cylindrica* (TCC2) was widely distributed along the coastline of the Indian Ocean, indicative of its long-distance dispersal ability spanning the Indian and Atlantic Ocean (Supplementary Table S4). The other three species in the *T. cylindrica* group might be endemic in the Pacific Ocean. TCC4 was only found in southern Taiwan and northern Luzon, Philippines, and UTC1 was only found in Jeju, Korea. Similarly, *T. confertus* (TC) was only found in southern Taiwan. Within TFC, TFC1 was primarily found in the Philippines. TFC2 and TFC3 were distributed in a much wider geographic range spanning the Indo-Pacific Ocean. Overall, TCG possesses higher species diversity and wider geographic distribution than TFC. Species in TFC is largely restricted to the subtropical and tropical areas, whereas species in TCG can inhabit in temperate regions (e.g. TJ and UTC1). Except for TCC1 and TJ, members in TFC have a wider distribution than those in TCG (Supplementary Table S4). It is also noted that species diversity was low at each sampling location, ranging between one and three species per site (Supplementary Table S4), indicative of the difficulty of collecting multiple *Tricleocarpa* species at one site.

Extrapolation of extant *Tricleocarpa* diversity

To quantify the sampling effort on the species richness of *Tricleocarpa* in the Central Indo-Pacific region, we applied the asymptote function to examine the current sampling effort using the online software iNEXT (see Materials and Methods for details). The best-fit unsampled species reached about 11 when extrapolated localities were added up to about threefold of reference sample size (Fig. 37; Supplementary Table S5). The upper limit of 95% bootstrap confidence for the extrapolated species richness was estimated to reach about 15, suggesting that a continuous sampling effort from

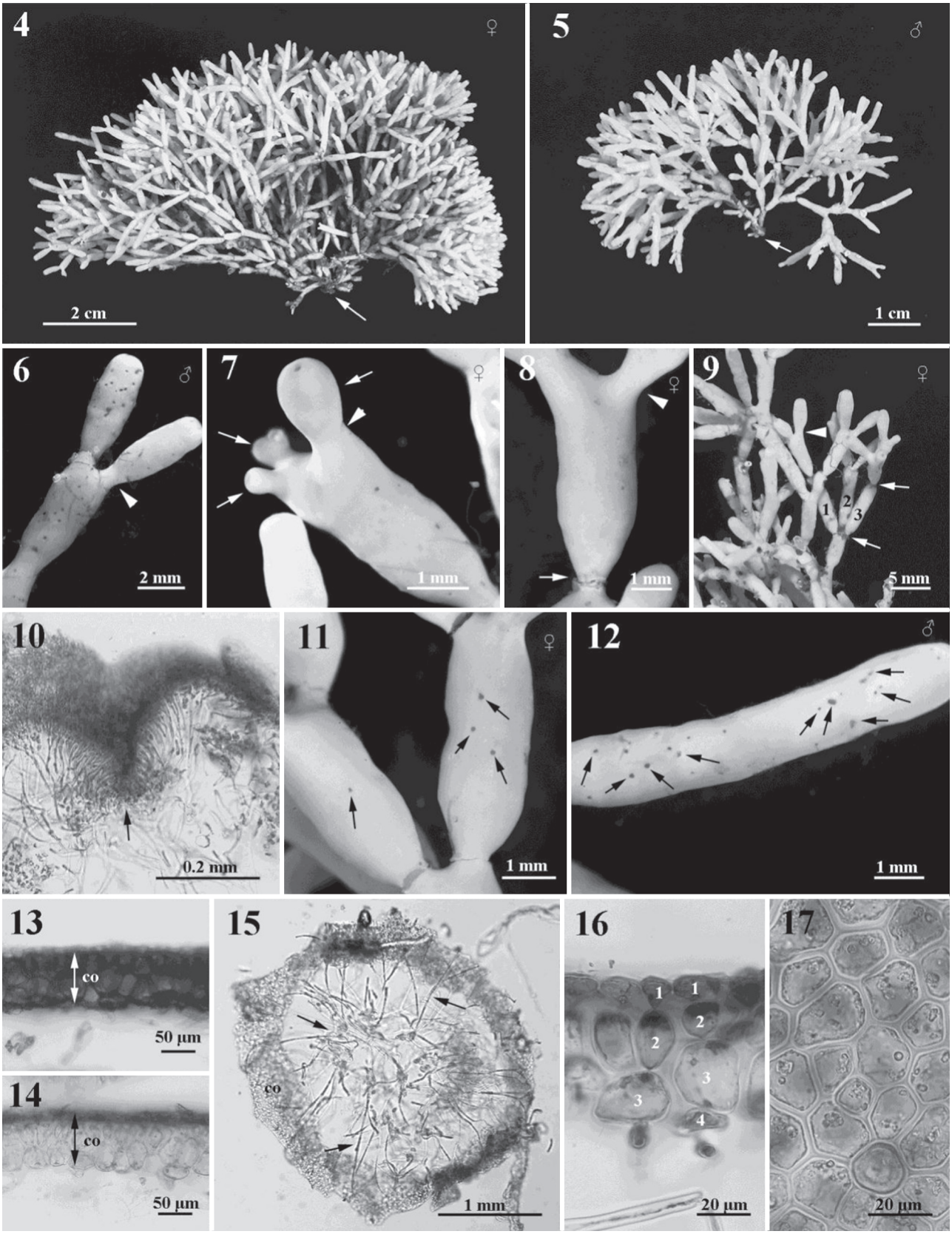

Figs 4–17. *Tricleocarpa confertus* S.-L. Liu & S.-M. Lin. Habit and vegetative structure (Figs 4, 7–9, 11, 13–14, 16–17: TUNG14033.4; XiaoLiuQiu Island, Taiwan; Figs 5–6, 12: TUNG14033.5, XiaoLiuQiu Island, Taiwan; Figs 10, 15: TUNG05010, Lanyu Island, Taiwan). **Fig. 4**. A female plant showing the articulated and moniliform branching pattern with a small discoid holdfast (arrow). **Fig. 5**. A male plant showing the articulated and moniliform branching pattern with a small discoid holdfast (arrow). **Fig. 6**. The terminal portion of a male thallus showing dichotomous branches with apparent constriction at the basal region of internode (arrowhead). **Fig. 7**. The terminal portion of a female thallus showing trichotomous branches (arrows) with distinct constricted region at the basal part of internode (arrowhead). **Fig. 8**. Internode showing the triangular internode, the constricted region at the basal region of internode (arrowhead), and the breakage at node (arrow). **Fig. 9**. Close-up of branches showing the articulated and moniliform

(*continued*)

more localities would increase the chance of discovering new *Tricleocarpa* species in the Central Indo-Pacific region, but with lower efficacy. Compared with the currently sampled species number from the Central Indo-Pacific region, the coverage of species richness (=sample coverage) might already reach 95% (Fig. 37; Supplementary Table S5), suggestive of a high sampling coverage of *Tricleocarpa* species richness in the Central Indo-Pacific region (Fig. 37).

DISCUSSION

With the help of advanced statistical analytical tools, we reassessed the species-level diversity of *Tricleocarpa* with the emphasis on the Indo-Pacific region. Based on two different loci (*rbc*L and COI-5P), molecular analyses revealed hidden species diversity of *Tricleocarpa*, ranging between 13 and 14 ESUs in *rbc*L and between 14 and 16 ESUs in COI-5P. In contrast to the observations made by Vieira *et al*. (2014), our results revealed that the GMYC model yielded more conservative results than those of SPN- and ABGD-based approaches. In addition, higher number of ESUs derived from COI-5P are probably due to higher rate of mutation accumulation in COI-5P in *Tricleocarpa* (Wiriyadamrikul *et al*. 2013*a*; Supplementary Table S4). Loci with a higher rate of mutation accumulation can capture more recent speciation events or population differentiation events in seaweeds as indicated by Payo *et al*. (2013) and Silberfeld *et al*. (2013). However, few putative species revealed by different single-locus algorithmic methods (e.g. the subdivisions of the TCC4 and TFC3 clades) received weaker support when using a validation approach – the two-gene Bayesian species delimitation analysis. Although the DNA-based, algorithmic species delimitation can be inaccurate when intraspecific variation is not well sampled (reviewed in Carstens *et al*., 2013), our diversity estimation should be conservative for several reasons. First of all, the 12 clusters determined by the combination of different algorithmic approaches agreed well with 12 well-separated ESUs in our phylogenetic analyses, further supporting their genetic cohesion of being distinct ESUs. Second, an *rbc*L sequence divergence of < 0.5% was considered as the cutoff for the species boundary in Galaxauraceae (e.g. Kurihara *et al*., 2005). The interspecific *rbc*L divergence for the majorities of ESUs in our species delimitation greatly exceeds such cutoff. We are aware that results of this study should be treated as a preliminary hypothesis and need to be tested further. Nevertheless, the biological relevance of some ESUs delineated by our analyses is supported by the morphological evidence. For instance, two ESUs that were recently described as two new species, *T. jejuensis* from northwestern Pacific region and *T. natalensis* from South Africa provides further support for our species delimitation. The new species, *T. confertus*, described in this study further justifies the biological relevance in our species delimitation outcome.

Wiriyadamrikul *et al*. (2013*a*) suggested that the genus *Tricleocarpa* contains at least five genetically distinct species in the Central Indo-Pacific region, including *T. cylindrica, T. fragilis, T. jejuensis* and two uncharacterized species. Extending their findings, our molecular analyses revealed additional species diversity in *Tricleocarpa*, which comprised of at least 10 species occurring in the Central Indo-Pacific region (by excluding UTC2 and TN). The main difference between Wiriyadamrikul *et al*. (2013*a*) and our study is the ESU subdivision of *T. fragilis* and *T. cylindrica* complexes. Both studies congruently suggest the inefficacy of diversity capture in *Tricleocarpa* if the species delimitation is solely based on morphological data. Recently, a growing body of molecular works has demonstrated that the species diversity of seaweeds is largely unexplored. For instance, Payo *et al*. (2013) demonstrated such a situation occurring in the genus *Portieria* Zanardini which shows a highly intra-archipelagic endemism and contains at least 21 cryptic species based on three-gene sequence analyses. The other two examples are the demonstration of many cryptic species in *Padina* Adanson and *Lobophora* J. Agardh using two-gene and three-gene molecular analyses (Silberfeld *et al*., 2013; Vieira *et al*., 2014). Echoed with Dijoux *et al*. (2014) who found new lineages and new species in *Asparagopsis* Montagne based on three-gene molecular analyses, our case study

Figs 4–17. Continued

branching pattern (arrows), trichotomous branches (numbered 1, 2 and 3), and apparent constricted region at the basal part of internode (arrowhead). **Fig. 10**. Longitudinal section through the terminal portion of a branch showing the apical meristem with numerous slender cortical filaments (arrow). **Fig. 11**. Close-up of ostioles of cystocarp conceptacles (arrows). **Fig. 12**. Close-up of ostioles of male conceptacles (arrows). **Fig. 13**. Cross-section through a branch showing the deposition of calcified crystals in the intercellular space region in the cortical layer (co). **Fig. 14**. Cross-section through a branch showing the cortical layer (co) after decalcification. **Fig. 15**. Cross-section through a branch showing the outer layer of cortical region (co) and the central medullary filaments (arrows). **Fig. 16**. Close-up of cross-section through a branch showing 3- or 4-celled cortical structures. Numbers indicate the different layers of cortical cells. **Fig. 17**. Surface view of a branch showing 4- to 7-sided polygonal outermost cortical cells. Scale bars = 2 cm (Fig. 5), 1 cm (Fig. 6), 2 mm (Fig. 7), 1 mm (Figs 8–10, 12–13, 16), 0.2 mm (Fig. 11), 50 μm (Figs 14–15) and 20 μm (Figs 17–18).

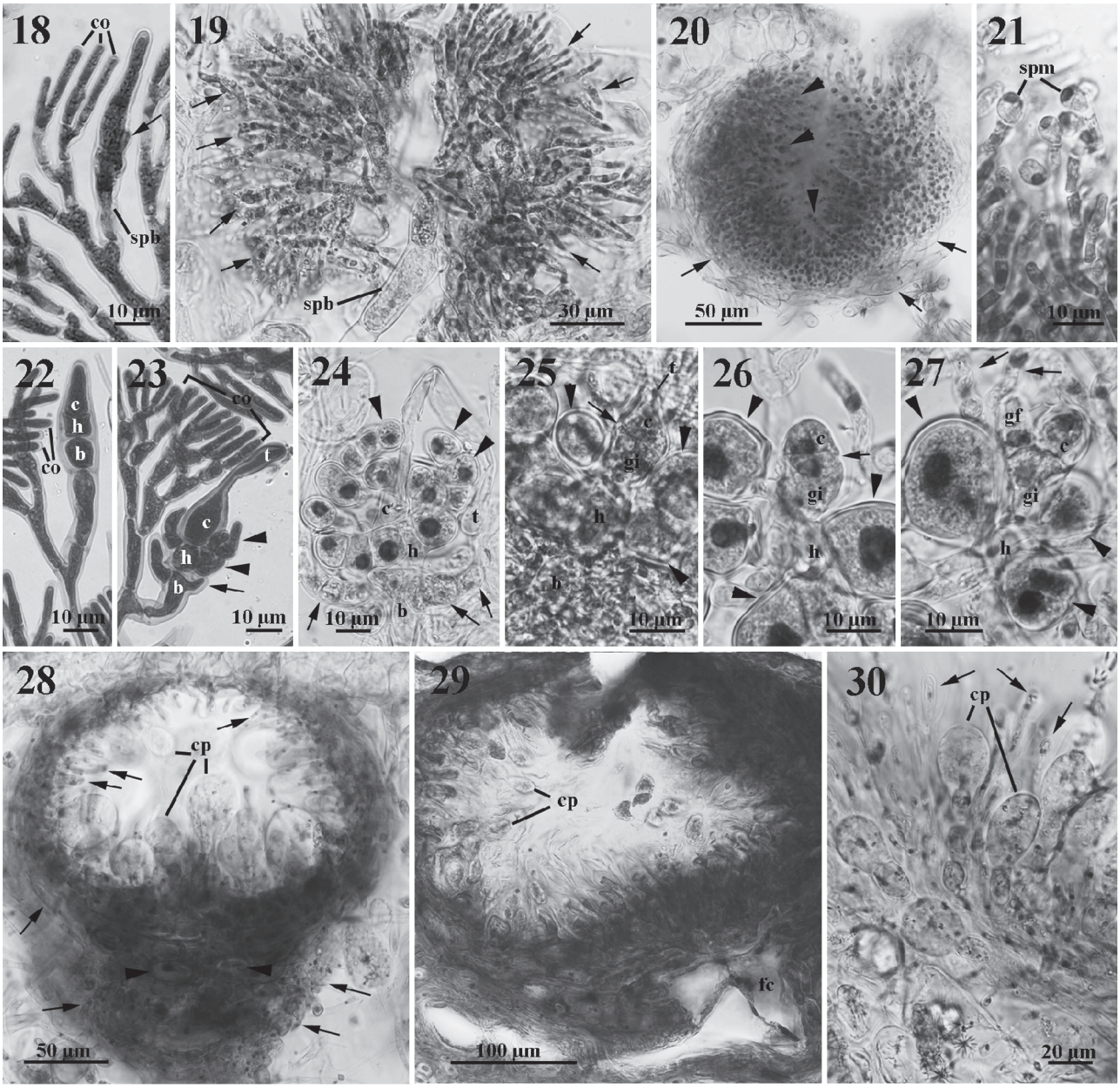

Figs 18–30. *Tricleocarpa confertus* S.-L. Liu & S.-M. Lin. Development of male and female structures (Figs 18–21: TUNG14033.5, XiaoLiuQiu Island, Taiwan; Figs 22–30: TUNG14033.4). **Fig. 18**. Spermatangial branch (spb) borne through the replacement of one of the dichotomous cortical filaments (co) and showing the production of young spermatangial filament initial (arrow). **Fig. 19**. Spermatangial branch (spb) bearing several primarily spermatangial filaments (arrows) over the course of the male conceptacle development. **Fig. 20**. Cross-section through an immature spermatangial conceptacle showing primary (arrows) and secondary spermatangial filaments (arrowheads). Note that the primary spermatangial filaments have formed the peripheral layer of the spermatangial conceptacle. **Fig. 21**. Spermatangia (spm) terminally borne on the secondary spermatangial filaments. **Fig. 22**. Carpogonial branch initial borne through the replacement of the dichotomous cortical filaments (co), and showing carpogonium (c), hypogynous cell (h) and basal cell (b). **Fig. 23**. Young carpogonial branch on the cortical filaments (co) showing carpogonium (c) with trichogyne (t), hypogynous cell (h) bearing two sterile branches (arrowheads), and basal cell (b) bearing two sterile branches (arrow). **Fig. 24**. Developed carpogonial branch showing carpogonium (c) with elongated trichogyne (t), hypogynous cell (h) producing three enlarged sterile branches (arrowheads), and basal cell (b) bearing sterile filaments (arrows). **Fig. 25**. Post-fertilized carpogonial branch showing fertilized carpogonium (c) with degenerated trichogyne (t), gonimoblast initial (gi), hypogynous cell (h) with enlarged sterile cells (arrowheads), and basal cell (b) bearing numerous sterile filaments. Note that the gonimoblast initial was produced through a transverse division of fertilized carpogonium (arrow). **Fig. 26**. Post-fertilized carpogonial branch showing carpogonium (c), gonimoblast initial (gi) derived from a transverse division of carpogonium (arrow), and hypogynous cell (h) producing enlarged sterile cells with dark stained nuclei (arrowheads). **Fig. 27**. Post-fertilized carpogonial branch showing fertilized carpogonium (c), gonimoblast initial (gi) cut off the first cell of gonimoblast filament (gf), and hypogynous cell (h) bearing several enlarged sterile cells with dark stained nuclei (arrowheads). Note that the carpogonial branch was surrounded by the sterile filaments (arrows) from the basal cell. **Fig. 28**. Cross-section of young cystocarp showing pericarp (arrows) from the basal cell, enlarged sterile cells (arrowheads) from hypogynous cell, and carposporangia (cp) borne on the secondary gonimoblast filaments. **Fig. 29**. Cross-section of mature cystocarp showing carposporangia (cp) borne terminally on the gonimoblast filaments and a distinct fusion cell (fc) at the basal part of cystocarp. **Fig. 30**. Close-up of mature cystocarp showing carposporangia (cp) on the gonimoblast filaments and paraphyses (arrows) derived from the sterile filaments of the basal cell. Scale bars = 10 µm (Figs 19, 22, 23–28), 30 µm (Fig. 20), 50 µm (Figs 21, 29), 100 µm (Fig. 30) and 20 µm (Fig. 31).

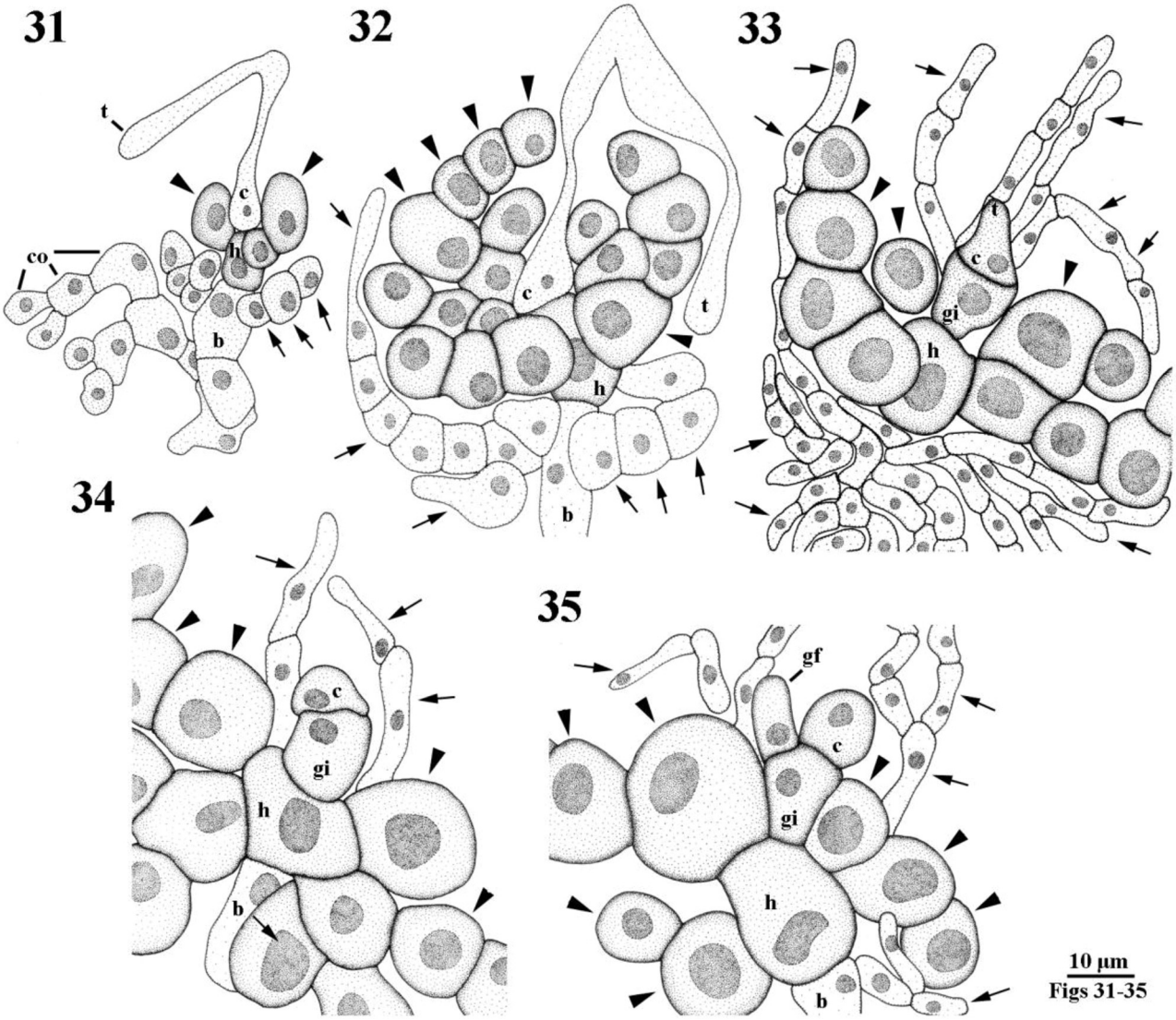

Figs 31–35. *Tricleocarpa confertus* S.-L. Liu & S.-M. Lin. Hand drawings of development of carpogonial branch (TUNG14033.4, XiaoLiuQiu Island, Taiwan). **Fig. 31**. Young carpogonial branch on the cortical filaments (co) showing carpogonium (c) with trichogyne (t), hypogynous cell (h) bearing two sterile branches (arrowheads), and basal cell (b) bearing two sterile branches (arrow). **Fig. 32**. Developed carpogonial branch showing carpogonium (c) with elongated trichogyne (t), hypogynous cell (h) producing three enlarged sterile branches (arrowheads), and basal cell (b) bearing sterile filaments (arrows). **Fig. 33**. Post-fertilized carpogonial branch showing fertilized carpogonium (c) with degenerated trichogyne (t), gonimoblast initial (gi), hypogynous cell (h) with enlarged sterile cells (arrowheads), and basal cell (b) bearing numerous sterile filaments. Note that the gonimoblast initial was produced through a transverse division of fertilized carpogonium (arrow). **Fig. 34**. Post-fertilized carpogonial branch showing carpogonium (c), gonimoblast initial (gi) derived from a transverse division of carpogonium (arrow), and hypogynous cell (h) producing enlarged sterile cells with dark stained nuclei (arrowheads). **Fig. 35**. Post-fertilized carpogonial branch showing fertilized carpogonium (c), gonimoblast initial (gi) cut off the first cell of gonimoblast filament (gf), and hypogynous cell (h) bearing several enlarged sterile cells with dark stained nuclei (arrowheads). Note that the carpogonial branch was surrounded by the sterile filaments (arrows) from the basal cell.

provides additional example of hidden diversity discovery through frequently samplings and two-gene molecular analyses.

Our phylogenetic analyses showed that tree topologies of *rbc*L+COI-5P are incongruent between the maximum likelihood and the Bayesian inferences. The ML tree of *rbc*L+COI-5P and the ML and Bayesian trees of COI-5P alone showed two monophyletic groups but the Bayesian inference failed to reveal such phylogenetic structure. Huisman & Borowitzka (1990) considered only two *Tricleocarpa* species occurring in Australia – *T. cylindrica* and *T. oblongata* (a later synonym of *T. fragilis*), which are separated by having different morphology of the innermost cortical cells (elongate versus compressed) and distinct patterns of gonimoblast filaments (diffused versus compact). In general, *T. confertus*, as well as *T. jejuensis* and *T. natalensis*, have elongate or slightly compressed innermost cortical cells and their gonimoblast filaments lining along the inner walls of

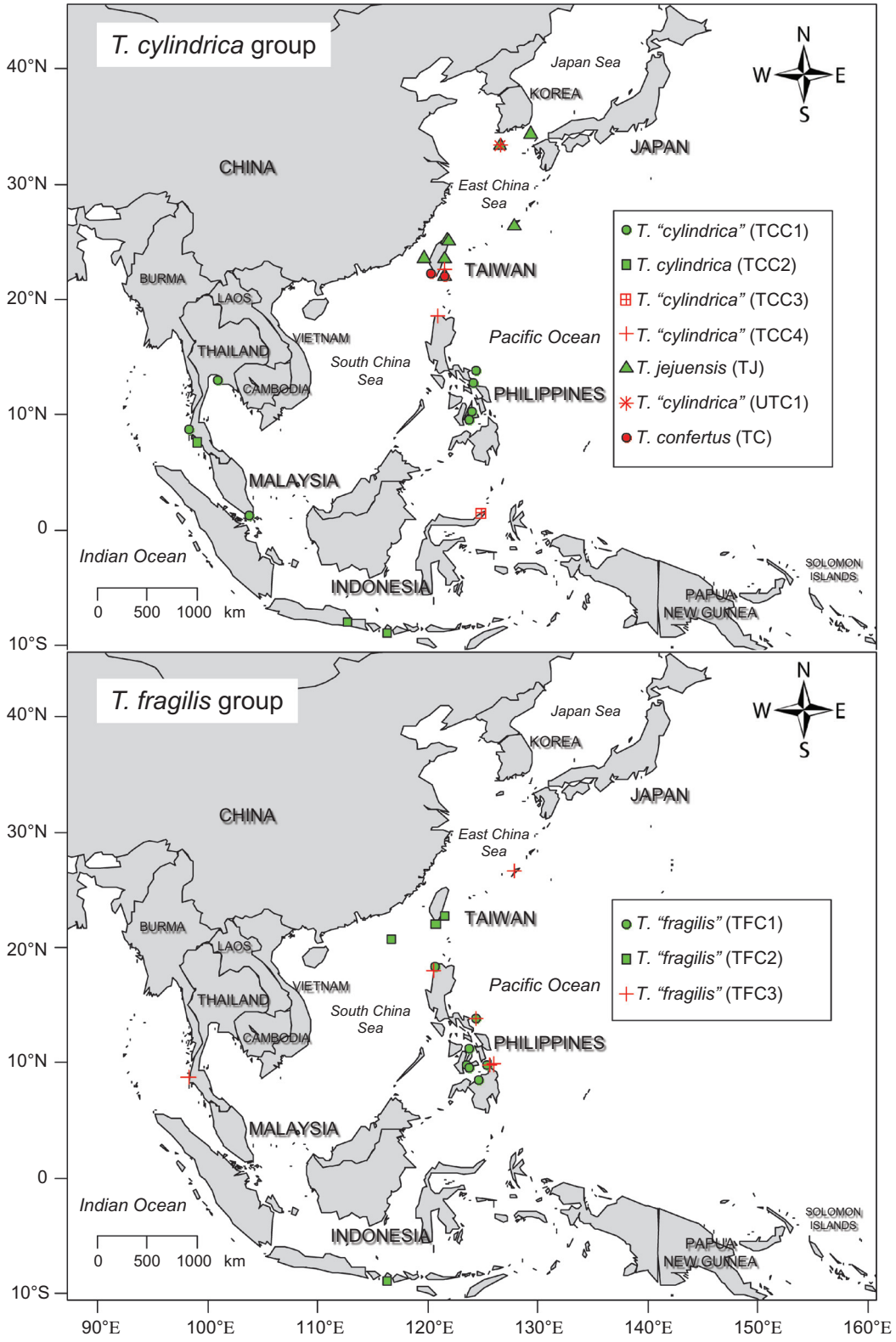

Fig. 36. Geographic distribution of *Tricleocarpa* species in the Central Indo-Pacific region. The geographic distribution of seven species in the *T. cylindrica* complex and three species in the *T. fragilis* complex are shown in the upper and lower panels respectively. The number of species are delineated by algorithm-based and phylogenetic inference (see Results for details).

the pericarps and intermixing with the paraphyses (Wiriyadamrikul *et al*., 2013*a*; this study), a situation similar to what was found in *T. cylindrica*. Thus, we classified *Tricleocarpa* species into two different species groups to circumscribe the 'two species' system proposed by Huisman & Borowitzka (1990) – the *T. cylindrica* and *T. fragilis* groups. From the parsimony point of view, the elongate innermost cortical cells and the gonimoblast filaments that line along the pericarp might be shared ancestral characters in the

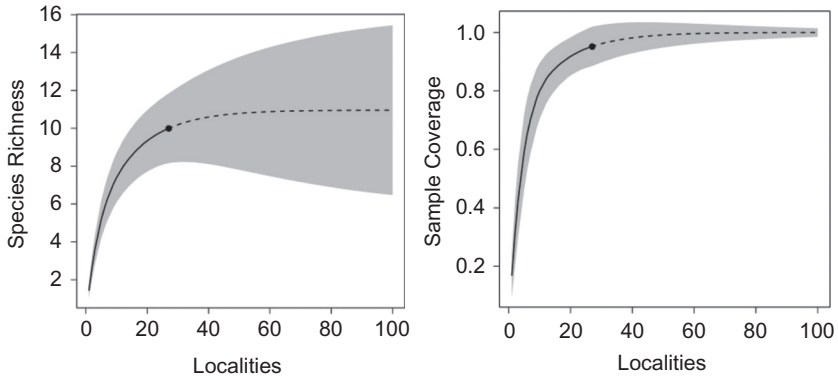

Fig. 37. Estimates of species richness of *Tricleocarpa* in the Central Indo-Pacific region using the online program iNEXT. The extrapolation of species richness and sample coverage beyond extant species diversity and sample coverage is derived from the simulated species accumulation curve of the known species frequency per site (black line) and the model fitting of the asymptote function (dash line). Grey area indicates the lower and upper limits of 95% bootstrap confidence interval.

T. cylindrica group, but the correlated evolution between traits and genes in *Tricleocarpa* will require further examinations by exploring other conserved barcode markers suitable for the resolution of higher taxonomic level (Janouškovec *et al*., 2013) or increasing taxon sampling (Zwickl & Hillis, 2002).

Although *T. confertus* shared a similar cystocarp development with other members in the *T. cylindrica* group, *T. confertus* can be characterized by articulated or moniliform branches with smooth surfaces and with constrictions at nodes, in which regions the branches are anti-triangular shape (Table 1). In contrast, the main axes in other *Tricleocarpa* species are cylindrical and dichotomously branched (e.g. section *Eugalaxaura* in Kjellman, 1900; Svedelius, 1945; Papenfuss *et al*., 1982; Huisman & Borowitzka, 1990; Wiriyadamrikul *et al*., 2013*a*). The constricted and moniliform branching pattern found in *T. confertus* is unusual in the genus *Tricleocarpa*. Although some species in *Dichotomaria* have moniliform branching pattern (e.g. *D. hommersandii* Liu & Lin and *D. obtusata* (Ellis & Solander) Lamarck (Liu *et al*., 2013; Wiriyadamrikul *et al*., 2014)) and can be confused with *T. confertus*, they do not have anti-triangular and trichotomous branches. In the past, the galaxauraceous samples were primarily collected from the intertidal or shallow subtidal region by picking or snorkelling. Since *T. confertus* can be only found in deeper subtidal areas, it is unlikely that this species can be seen without scuba diving. Overall, it is very straightforward to externally distinguish *T. confertus* from other *Tricleocarpa* species. It is possible that its biogeographic range will be much broader with more scuba-diving collections.

In Wiriyadamrikul *et al*. (2013*a*) and this study, four additional uncharacterized species in the *T. cylindrica* group (TCC1, TCC3, TCC4 and UTC1) were found in the Central Indo-Pacific region. When summarizing the species of *Galaxaura* that might be associated with *Tricleocarpa, Galaxaura conglutinata* Kjellman, *G. dimorpha* Kjellman, *G. eburnea* Kjellman and *G. fastigiata* Decaisne are the only four species with type localities in the Central Indo-Pacific region (Supplementary Table S5). To match these four species with our uncharacterized species in the *T. cylindrica* complex, *G. conglutinata, G. dimorpha* and *G. eburnea* can be excluded from further considerations because its gross morphology was shown to be close to *T. cylindrica* and *T. fragilis* (see discussion in Wiriyadamrikul *et al*., 2013*a*). The type locality of *G. fastigiata* is however questionable. Svedelius (1945) considered the specimens from Manila, the Philippines as the type of this entity. However, Papenfuss *et al*. (1982) suggested that Timor, Indonesia is the type locality for *G. fastigiata*. If the former one is accepted, the species identity of the TCC4 clade will be likely associated with *G. fastigiata* according to their biogeographic affinities. In contrast, the true *T. cylindrica* (TCC2) will be likely affiliated with *G. fastigiata* if the latter one is accepted. When Svedelius (1945) summarized the taxonomy of *Galaxaura* species attributed to Kjellman's section *Eugalaxaura*, he examined the lectotype of *G. fastigiata* (Voucher No.: Cuming 2241) and concluded 'the branches of *G. fastigiata* are generally narrower throughout than in *G. oblongata*, in natural condition or preserved in formalin hardly 1 mm in breadth, at the base at most 1.3 mm'. The specimen from Green Island, Taiwan (as TCC4) showed very slender branches throughout the thallus (≦ 1 mm) (data not shown), agreeing well with the description of *G. fastigiata* in Svedelius (1945). Without further morphological examinations in TCC4, we however defer the match of *G. fastigiata* with TCC4. TCC1 was largely restricted to the central Philippines. So far, no *Galaxaura* species has the type locality near that area, suggesting that this alga could be new to science. However, we are not able to evaluate this species unless more samples are available. TCC3 was found in Manado and Hawaii. Svedelius

(1953) recognized Hawaiian *Tricleocarpa* as *G. fastigiata*. Since the type locality of *G. fastigiata* is far away from these two locations and their sequences are different from TCC4, specimens from Hawaii should be characterized as a new species. UTC1 was only found in Jeju, Korea, suggesting that it can be another species new to science. However, the lack of sufficient samples delayed further taxonomic treatments for this entity (Wiriyadamrikul *et al*., 2013*a*). At present, we are unable to determine the true *T. fragilis* by the lack of authentic sequences from its type locality – the Caribbean Sea. A total of three putative species (TFC1, TFC2 and TFC3) were observed in the *T. fragilis* complex, indicative of the hidden species diversity in *T. fragilis*. Although several *Galaxaura* species might be affiliated with *T. fragilis*, none of them has type locality in the Central Indo-Pacific region (Supplementary Table S5). We therefore defer taxonomic matches between any *Galaxaura* species names and our three *T. fragilis* ESUs. Overall, the species identity for many *Tricleocarpa* species requires further examination by applying the integrative taxonomy approach.

Five out of 12 ESUs (*c*. 42%) showed the trans-oceanic geographic distribution spanning two oceanic basins (Supplementary Table S2), including three species in the *T. cylindrica* group (TCC1, TCC2 and TJ) and two species in the *T. fragilis* complex (TFC2 and TFC3). Except for TCC2 that was distributed to the Indian Ocean and Atlantic Ocean, the other four ESUs were distributed to the Indo-Pacific Ocean. Two possible explanations might account for such long-distance biogeographic patterns. One possibility is that these *Tricleocarpa* species have been introduced through human-mediated activities such as aquaculture or the release of ballast water as often seen in seaweeds as a review made by William & Smith (2007). The other possibility is the recent speciation events predating the Tethys Sea where the global tropical area was connected for the trans-oceanic dispersal of tropical seaweeds before the closure of the Mediterranean Sea (*c*. 12–19 Mya) and the Central American isthmus (*c*. 3–4 Mya). Analogous historical dispersal routes have been proposed in many tropical seaweeds (Verbruggen *et al*., 2009; Tronholm *et al*., 2012; Silberfeld *et al*., 2013). As no divergence rate is available for COI-5P in red algae and both *rbc*L and COI-5P are not suitable for molecular dating due to their non-neutral evolutionary fashion, we therefore defer the estimation of divergence time before any historical framework of biogeographic patterns for the genus *Tricleocarpa* can be proposed without the use of neutral markers (e.g. the intergenic spacer *cox2-3*; Zuccarello & West, 2002). Overall, the first scenario could be favoured in some cases. For instance, *T. cylindrica* from Guadeloupe and Malang, Indonesia shared 100% identical *rbc*L sequences, which hardly account for the long-distance dispersal by historical events. In contrast to the above-mentioned ESUs, other *Tricleocarpa* ESUs are only known from a rather smaller geographic range in the West Pacific region such as *T. confertus*, TCC4 and UTC1. However, it might be possible that these species occur in other regions of the Pacific region when more sampling can be made.

The diversification of marine organisms can be caused by several mechanisms, such as allopatric speciation through the physical barriers (e.g. ocean currents), peripatric speciation by founder events, or sympatric speciation by niche differentiation, as reviewed by Paulay & Meyer (2002). In *Tricleocarpa*, the restricted northwestern Pacific distribution of two species, *T. jejuensis* and the uncharacterized *T.* '*cylindrica*'(UTC1), from Jeju, Korea may be explained by the founder effect speciation events as suggested by Wiriyadamrikul *et al*. (2013*a*). Alternatively, the speciation event might be facilitated by the isolation of ocean current as *T. jejuensis* is largely restricted to temperate northern Pacific realm. Both founder effect and ocean current barrier were observed in the brown algal genera, *Dictyota* Lamouroux (Tronholm *et al*., 2012) and *Padina* (Silberfeld *et al*., 2013). Speciation via niche or micro-environmental differentiation along intertidal or subtidal zones might also play another important role in the species diversification of *Tricleocarpa*. For instance, *T. confertus* was only found subtidally, suggesting that its speciation event might be explained through an adaptation to a deeper/cooler water environment in sub- or tropical regions. Speciation events occurred along the intertidal and subtidal zones have been also found in other temperate seaweeds in the brown algal genera, *Dictyota* (Tronholm *et al*., 2010) and *Fucus* Linnaeus (Zardi *et al*., 2011). Fine-scale temporal and spatial sampling would help to elucidate the speciation mechanisms of *Tricleocarpa* in the future.

ACKNOWLEDGEMENTS

This study was financially supported by grants from Ministry of Science and Technology (MOST), Taiwan (102-2621-B-029-002 & 103-2611-M-029 -001) to SLL and MOST grants (102-2621-B-019-001 & 102-2811-B-019-001) to SML. The authors thank P.-H. Lai, T.-Y. Hsieh and Y.-S. Chiou for assisting with DNA sequencing and specimen sorting.

DISCLOSURE STATEMENT

No potential conflict of interest was reported by the author(s).

SUPPLEMENTARY INFORMATION

The following supplementary material is accessible via the Supplementary Content tab on the article's online page at http://dx.doi.org/10.1080/09670262.2015.1076892

Supplementary table S1. List of codes of evolutionary species units (ESU), species name, collection information/reference, and GenBank accession number.

Supplementary table S2. Results of the Generalized Mixed Yule-Coalescent (GMYC) analyses under the single threshold model.

Supplementary table S3. Results of the Automated Barcode Gap Discovery (ABGD) analyses.

Supplementary table S4. Occurrence of 12 *Tricleocarpa* species analysed in this study. Number indicates the number of specimens at each collection locality.

Supplementary table S5. List showing the extrapolation of species richness and sample coverage beyond the extant species richness and sample coverage up to about three-fold of reference sample size (endpoint = 100).

Supplementary table S6. Interspecific and intraspecific (as italic) uncorrected pairwise *P*-distance (%) of 12 *Tricleocarpa* ESUs for the *rbc*L dataset and the COI-5P dataset.

Supplementary table S7. List of species names of *Galaxaura* that are associated with the genus *Tricleocarpa* in the literature.

Supplementary figure S1. Phylogram of concatenated *rbc*L and COI-5P of all available *Tricleocarpa* sequences based on the Bayesian inference.

AUTHOR CONTRIBUTIONS

S.L. Liu: original concept, field collection, analysis of molecular data, drafting and editing manuscript; S.M. Lin: original concept, field collections, editing manuscript; P.C. Chen: molecular experiments, editing manuscript.

REFERENCES

Abbott, I.A. (1999). *Marine red algae of Hawaiian Islands*, 63–75. Bishop Museum Press, Honolulu, HI.

Carstens, B.C., Pelletier, T.A., Reid, N.M. & Satler, J.D. (2013). How to fail at species delimitation. *Molecular Ecology*, **22**: 4369–4383.

Chao, A. & Jost, L. (2012). Coverage-based rarefaction and extrapolation: standardizing samples by completeness rather than size. *Ecology*, **93**: 2533–2547.

Clement, M., Posada, D. & Crandall, K.A. (2000). TCS: a computer program to estimate gene genealogies. *Molecular Ecology*, **9**: 1657–1659.

Colwell, R.K., Chao, A., Gotelli, N.J., Lin, S.Y., Mao, C.X., Chazdon, R.L. & Longino, J.T. (2012). Models and estimators linking individual-based and sample-based rarefaction, extrapolation and comparison of assemblages. *Journal of Plant Ecology*, **5**: 3–21.

Dijoux, L., Viard, F. & Payri, C. (2014). The more we search, the more we find: discovery of a new lineage and a new species complex in the genus *Asparagopsis*. *PLoS ONE*, **9**: e103826.

Drummond, A.J. & Rambaut, A. (2007). BEAST: Bayesian evolutionary analysis by sampling trees. *BMC Evolutionary Biology*, **7**: 214.

Drummond, A.J., Ho S.Y.W., Phillips, M.J. & Rambaut, A. (2006). Relaxed phylogenetics and dating with confidence. *PLoS Biology*, **4**: 699–710.

Felsenstein, J. (1985). Confidence limits on phylogenies: an approach using bootstrap. *Evolution*, **39**: 783–791.

Freshwater, D.W. & Rueness, J. (1994). Phylogenetic relationships of some European *Gelidium* (Gelidiales, Rhodophyta) species based on *rbc*L nucleotide sequence analysis. *Phycologia*, **33**: 187–194.

Fujisawa, T. & Barraclough, T.G. (2013). Delimiting species using single-locus data and the Generalized Mixed Yule Coalescent approach: a revised method and evaluation on simulated data sets. *Systematic Biology*, **62**: 707–724.

Geraldino, P.J.L., Yang, E.C. & Boo, S.M. (2006). Morphology and molecular phylogeny of *Hypnea flexicaulis* (Gigartinales, Rhodophyta) from Korea. *Algae*, **21**: 417–423.

Hart, M.W. & Sunday, J. (2007). Things fall apart: biological species form unconnected parsimony networks. *Biology Letter*, **3**: 509–512.

Hsieh, T.C., Ma, K.H. & Chao, A. (2013). iNEXT online: interpolation and extrapolation (Version 1.3.0) [Software]. Available from http://chao.stat.nthu.edu.tw/blog/software-download/.

Huisman, J.M. (2006). *Algae of Australia: Nemaliales*. Australian Biological Resources Study, Canberra; CSIRO Publishing, Melbourne.

Huisman, J.M. & Borowitzka, M.A. (1990). A revision of the Australian species of *Galaxaura* (Rhodophyta, Galaxauraceae), with a description of *Tricleocarpa* gen. nov. *Phycologia*, **29**: 150–172.

Huisman, J.M. & Townsend, R.A. (1993). An examination of Linnaean and pre-Linnaean taxa referable to *Galaxaura* and *Tricleocarpa* (Galaxauraceae, Rhodophyta). *Botanical Journal of the Linnean Society*, **113**: 95–101.

Huisman, J.M., Harper, J.T. & Saunders, G.W. (2004). Phylogenetic study of the Nemaliales (Rhodophyta) based on large-subunit ribosomal DNA sequence supports segregation of the Scinaiaceae fam. nov. and resurrection of *Dichotomaria* Lamarck. *Phycological Research*, **52**: 224–234.

Janouškovec, J., Liu, S.L., Martone, P.T., Carré, W., Leblanc, C., Collén, J. & Keeling, P.J. (2013). Evolution of red algal plastid genomes: ancient architectures, introns, horizontal gene transfer, and taxonomic utility of plastid markers. *PLoS ONE*, **8**: e59001.

Kekkonen, M. & Hebert, P.D.N. (2014). DNA barcode-based delineation of putative species: efficient start for taxonomic workflows. *Molecular Ecology Resources*, **14**: 706–715.

Kjellman, F.R. (1900). Om floridé-slägtet *Galaxaura* dess organografi och systematic. *Kungliga Svenska Vetenskapsakademiens Handlingar*, **33**: 1–109.

Kurihara, A., Arai, S., Shimada, S. & Masuda, M. (2005) The conspecificity of *Galaxaura apiculata* and *G. hystrix* (Nemaliales, Rhodophyta) inferred from comparative morphology and rbcL and ITS sequences. *European Journal of Phycology*, **40**: 39–52.

Lanfear, R., Calcott, B., Ho, S.Y.W. & Guindon, S. (2012). PartitionFinder: combined selection of partitioning schemes and substitution models for phylogenetic analyses. *Molecular Biology and Evolution*, **29**: 1695–1701.

Leaché, A.D. & Fujita, M.K. (2010). Bayesian species delimitation in west African forest geckos (*Hemidactylus fasciatus*). *Proceedings of Royal Society B*, **277**: 3071–3077.

Leliaert, F., Verbruggen, H., Vanormelingen, P., Steen, F., López-Bautista, J.M., Zuccarello, G.C. & De Clerk, O. (2014). DNA-based species delimitation in algae. *European Journal of Phycology*, **49**: 179–196.

Lin, S.M., Fredericq, S. & Hommersand, M.H. (2001). Systematics of the Delesseriaceae (Ceramilaes, Rhodophyta) based on large subunit rDNA and *rbc*L sequences, including the Phycodryoideae, subfam. nov. *Journal of Phycology*, **37**: 881–899.

Liu, S.L., Lin, S.M. & Wang, W.L. (2013). Molecular phylogeny of the genus *Dichotomaria* (Galaxauraceae, Rhodophyta) from the Indo-Pacific region, including a new species *D. hommersandii* from South Africa. *European Journal of Phycology*, **48**: 221–234.

Monaghan, M.T., Wild, R., Elliot, M., Fujisawa, T., Balke, M., Inward, D.J., Lees, D.C., Ranaivosolo, R., Eggleton, P., Barraclough, T.G. & Vogler, A.P. (2009). Accelerated species inventory on Madagascar using coalescent-based models of species delineation. *Systematic Biology*, **58**: 298–311.

Papenfuss, G.F. & Chiang, Y.M. (1969). Remarks on the taxonomy of *Galaxaura* (Nemaliales, Chaetangiaceae). *Proceedings of the International Seaweed Symposium*, **6**: 303–314.

Papenfuss, G.F., Mshigeni, K.E. & Chiang, Y.M. (1982). Revision of the red algal genus *Galaxaura* with special reference to the species occurring in the western Indian Ocean. *Botanica Marina*, **25**: 401–444.

Paulay, G. & Meyer, C. (2002). Diversification in the tropical Pacific: comparisons between marine and terrestrial systems. *Integrative and Comparative Biology*, **42**: 922–934.

Payo, D.A., Leliaert, F., Verbruggen, H., D'hondt, S., Calumpong, H.P. & De Clerk, O. (2013). Extensive cryptic species diversity and fine-scale endemism in the marine red alga *Portieria* in the Philippines. *Proceedings of the Royal Society B*, **280**: 20122660.

Pons, J., Barraclough, T.G., Gomez-Zurita, J., Cardoso, A., Duran, D.P., Hazall, S., Kamoun, S., Sumlin, W.D. & Vogler, A.P. (2006). Sequence-based species delimitation for the DNA taxonomy of undescribed insects. *Systematic Biology*, **55**: 595–609.

Puillandre, N., Lambert, A., Brouillet, S. & Achaz, G. (2012). ABGD, Automatic Barcode Gap Discovery for primary species delimitation. *Molecular Ecology*, **21**: 1864–1877.

Rambaut, A. & Drummond, A.J. (2007). Tracer v. 1.4. (http://best.bio.ed.ac.uk/Tracer).

Rannala, B. & Yang, Z. (2003). Bayes estimation of species divergence times and ancestral population sizes using DNA sequences from multiple loci. *Genetics*, **164**: 1645–1656.

Ronquist, F., Teslenko, M., van der Mark, P., Ayres, D.L., Darling, A., Höhna, S., Larget, B., Liu, L., Suchard, M.A. & Huelsenbeck, J.P. (2012). MrBayes 3.2: efficient Bayesian phylogenetic inference and model choice across a large model space. *Systematic Biology*, **61**: 539–542.

Saunders, G.W. & Moore, T.E. (2013). Refinements for the amplification and sequencing of red algal DNA barcode and RedToL phylogenetic markers: a summary of current primers, profiles and strategies. *Algae*, **28**: 31–43.

Schlick-Steiner, B.C., Steiner, F.M., Seifert, B., Stauffer, C., Christian, E. & Crozier, R.H. (2010). Integrative taxonomy: a multisource approach to exploring biodiversity. *Annual Review of Entomology*, **55**: 421–438.

Sherwood, A.R., Kurihara, A., Conklin, K.Y., Sauvage, T. & Presting, G.G. (2010). The Haiwaiian Rhodophyta biodiversity survey (2006–2010): a summary of principal findings. *BMC Plant Biology*, **10**: 258.

Silberfeld, T., Bittner, L., Fernández-Garcia, C., Cruaud, C., Rousseau, F., de Reviers, B., Leliaert, F., Payri, C.E. & De Clerk, O. (2013). Species diversity, phylogeny and large scale biogeographic patterns of the genus *Padina* (Phaeophyta, Dictyotales). *Journal of Phycology*, **49**: 130–142.

Stamatakis, A. (2006). RAxML-VI-HPC: maximum likelihood-based phylogenetic analyses with thousands of taxa and mixed models. *Bioinformatics*, **22**: 2688–2690.

Svedelius, N. (1945). Critical notes on some species of *Galaxaura* from Ceylon. *Arkiv för Botanik Uppsala*, **32A**: 1–74.

Svedelius, N. (1953). Critical studies on some species of *Galaxaura* from Hawaii. *Nova Acta Regiae Societatis Scientiarum Upsaliensis, series 4*, **15**: 1–92.

Tamura, K., Stecher, G., Peterson, D., Filipski, A. & Kumar, S. (2013). MEGA6: Molecular Evolutionary Genetics Analysis version 6.0. *Molecular Biology and Evolution*, **30**: 2725–2729.

Templeton, A.R., Crandall, K.A. & Sing, C.F. (1992). A cladistic analysis of phenotypic associations with haplotypes inferred from restriction endonuclease mapping and DNA sequence data. III. Cladogram estimation. *Genetics*, **132**: 619–633.

Tronholm, A., Sansón, M., Afonso-Carrillo, J., Verbruggen, H. & De Clerck, O. (2010). Niche partitioning and the coexistence of two cryptic *Dictyota* (Dictyotales, Phaeophyceae) species from the Canary Islands. *Journal of Phycology*, **46**: 1075–1087.

Tronholm, A., Leliaert, F., Sansón, M., Afonso-Carrillo, J., Tyberghein, L., Verbruggen, H. & De Clerk, O. (2012). Contrasting geographical distributions as a result of thermal tolerance and long-distance dispersal in two allegedly widespread tropical brown algae. *PLoS ONE*, **7**: e30813.

Verbruggen, H., Leliaert, F., Maggs, C.A., Shimada, S., Schils, T., Provan, J., Booth, D., Murphy, S., De Clerck, O., Littler, D.S., Littler, M.M. & Coppejans, E. (2007). Species boundaries and phylogenetic relationships within the green algal genus *Codium* (Bryopsidales) based on plastid DNA sequences. *Molecular Phylogenetics and Evolution*, **44**: 240–254.

Verbruggen, H., Tyberghein, L., Pauly, K., Van Nieuwenhuyse, K., Vlaeminck, C., Kooistra, W., Leliaert, F. & De Clerk, O. (2009). Macroecology meets macroevolution: evolutionary niche dynamics in the marine green alga *Halimeda*. *Global Ecology and Biogeography*, **18**: 393–405.

Vieira, C., D'Hondt, S., De Clerck, O. & Payri, C.E. 2014. Toward an inordinate fondness for stars, beetles and *Lobophora*? Species diversity of the genus *Lobophora* (Dictyotales, Phaeophyceae) in New Caledonia. *Journal of Phycology*, **50**: 1101–1119.

Wang, W.L., Liu, S.L. & Lin, S.M. (2005). Systematics of the calcified genera of the Galaxauraceae (Nemaliales, Rhodophyta) with an emphasis on Taiwan species. *Journal of Phycology*, **41**: 685–703.

William, S.L. & Smith, J.E. (2007). A global review of the distribution, taxonomy, and impacts of introduced seaweeds. *Annual Review of Ecology, Evolution, and Systematics*, **38**: 327–359.

Wiriyadamrikul, J., Geraldino, J.L., Huisman, J.M., Lewmanomont, K. & Boo, S.M. (2013a). Molecular diversity of the calcified red algal genus *Tricleocarpa* (Galaxauraceae, Nemaliales) with the description of *T. jejuensis* and *T. natalensis*. *Phycologia*, **52**: 338–351.

Wiriyadamrikul, J., Lewmanomont, K. & Boo, S.M. (2013b). Molecular diversity and morphology of the genus *Actinotrichia* (Galaxauraceae, Rhodophyta) from the western Pacific, with a new record of *A. robusta* in the Andaman Sea. *Algae*, **28**: 53–62.

Wiriyadamrikul, J., Wynne, M.J. & Boo, S.M. (2014). Phylogenetic relationships of *Dichotomaria* (Nemaliales, Rhodophyta) with the proposal of *Dichotomaria intermedia* (R.C.Y. Chou) comb. nov. *Botanica Marina*, **57**: 27–40.

Wittmann, W. (1965). Aceto-iron-haematoxylin-chloral hydrate for chromosome staining. *Stain Technology*, **40**: 161–164.

Yang, E.C., Kim, M.S., Geraldino, P.J.L., Sahoo, D., Shin, J.A. & Boo, S.M. (2008). Mitochondrial *cox*1 and plastid *rbc*L genes of *Gracilaria vermiculophylla* (Gracilariaceae, Rhodophyta). *Journal of Applied Phycology*, **20**: 161–168.

Yang, Z. & Rannala, B. (2010). Bayesian species delimitation using multilocus sequence data. *Proceedings of the National Academy of Sciences USA*, **107**: 9264–9269.

Zardi, G.I., Nicastro, K.R., Canovas, F., Costa, J.F., Serrão, E.A. & Pearson, G.A. (2011). Adaptive traits are maintained on steep selective gradients despite gene flow and hybridization in the intertidal zone. *PLoS ONE*, **6**: e19402.

Zwickl, D.J. & Hillis, D. (2002). Increased taxon sampling greatly reduces phylogenetic error. *Systematic Biology*, **51**: 588–598.

Zuccarello, G.C. & West, J.A. (2002). Phylogeography of the *Bostrychia calliptera – B. pinnata* complex (Rhodomelaceae, Rhodophyta) and divergence rates based on nuclear, mitochondrial and plastid DNA markers. *Phycologia*, **41**: 49–60.